Electronic Supplementary Information

Chemical reduction of Ag^+ to Ag employing organic electron donors: Evaluation of the effect of Ag^+-mediated cytosine–cytosine base pairing on the aggregation of Ag nanoparticles

Takenori Dairaku,*[a] Rika Kawai,[a] Kanako Nozawa-Kumada,[b] Kentaro Yoshida,[a] Tetsuya Ono,[a] Yoshinori Kondo,[b] Jiro Kondo,[c] Akira Ono,[d] Yoshiyuki Tanaka,[e] and Yoshitomo Kashiwagi*[a]

[a] School of Pharmaceutical Sciences, Ohu University, 31-1 Misumido, Tomita-machi, Koriyama, Fukushima 963-8611, Japan

E-mail: t-dairaku@pha.ohu-u.ac.jp

E-mail: y-kashiwagi@pha.ohu-u.ac.jp

[b] Graduate School of Pharmaceutical Sciences, Tohoku University, 6-3 Aza-Aoba, Aramaki, Aoba-ku, Sendai, Miyagi 980-8578, Japan

[c] Department of Materials and Life Sciences, Faculty of Science and Technology, Sophia University, 7-1 Kioi-cho, Chiyoda-ku, Tokyo 102-8554, Japan

[d] Department of Material & Life Chemistry, Faculty of Engineering, Kangawa University, 3-27-1 Rokkakubashi, Kanagawa-ku, Yokohama, Kanagawa 221-8686, Japan

[e] Faculty of Pharmaceutical Sciences, Tokushima Bunri University, Yamashiro-cho, Tokushima 770-8514, Japan

*Corresponding authors

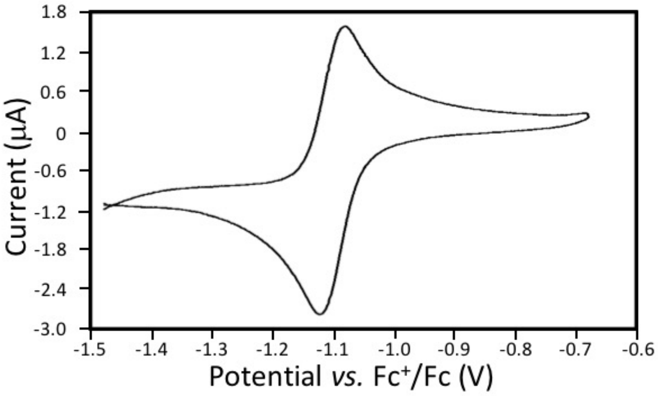

Fig. S1 Cyclic voltammogram of 30 mM tetrakis(dimethylamino)ethylene (TDAE) in DMSO containing 100 mM $NaNO_3$ as the supporting electrolyte. The scan rate was 0.01 V s^{-1}.

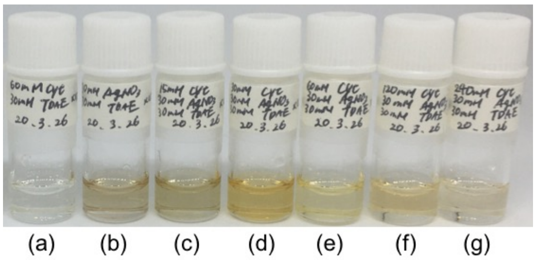

Fig. S2 Ten-fold dilutions of the solutions: (a) 6 mM cytidine/3 mM TDAE in DMSO and the supernatant fluids obtained from the centrifugation of cytidine:$AgNO_3$:TDAE molar ratios: (b) 0:1:1, (c) 0.5:1:1, (d) 1:1:1, (e) 2:1:1, (f) 4:1:1, and (g) 8:1:1. The solutions before dilution are shown in Fig. 2.

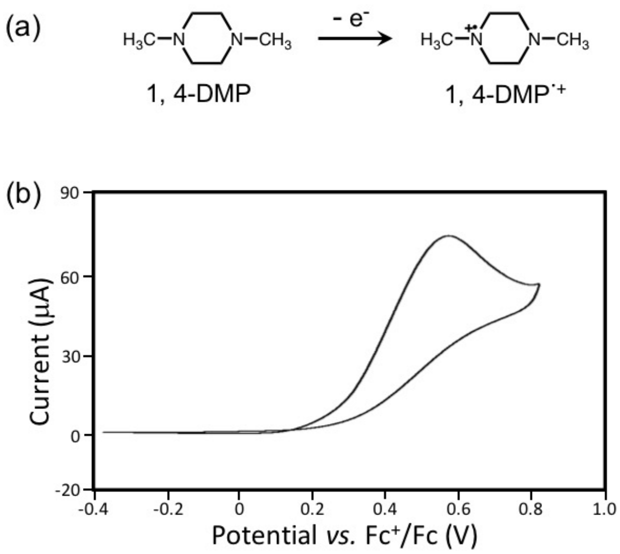

Fig. S3 (a) Chemical structures of 1, 4-DMP and its proposed oxidation states. (b) Cyclic voltammogram of 30 mM 1, 4-DMP in DMSO containing 100 mM $NaNO_3$ as a supporting electrolyte with a scan rate 0.01 V s^{-1}.

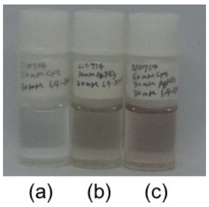

Fig. S4 Solution of (a) 30 mM 1, 4-DMP, (b) 30 mM $AgNO_3$ /30 mM 1, 4-DMP, and (c) 60 mM cytidine/30 mM $AgNO_3$ /30 mM 1, 4-DMP in DMSO.

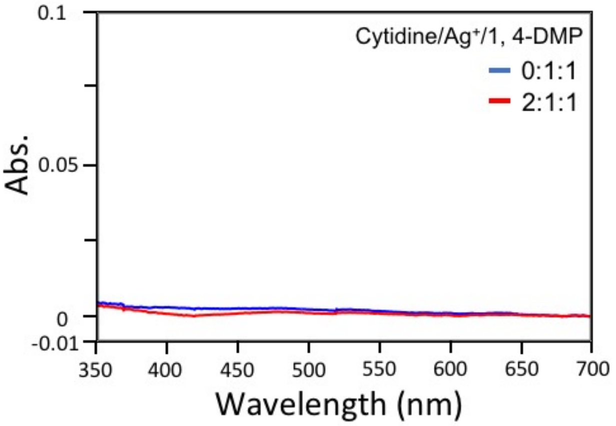

Fig. S5 UV–Vis spectra of the 10-fold diluted samples, which were obtained from solutions (b) and (c) (Fig. S4). The cytidine:$AgNO_3$:1, 4-DMP molar ratios were 0:1:1 (blue) and 2:1:1 (red).

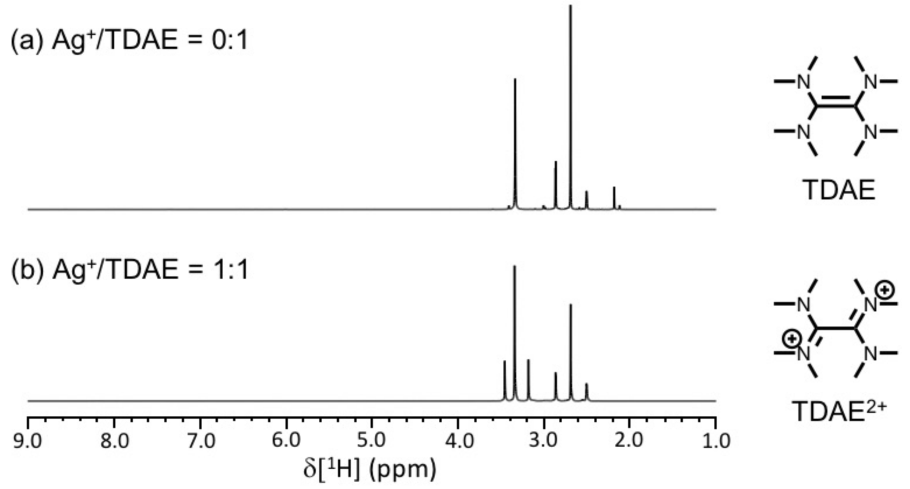

Fig. S6 1D ^{1}H NMR spectra (500 MHz) of (a) 30 mM TDAE and (b) the supernatant fluid that was obtained from centrifuging the 30 mM $AgNO_3$/30 mM TDAE solution in DMSO-d_6. In the presence of Ag^+, two new methyl proton signals appeared at 3.18 and 3.45 ppm. The 1D ^{1}H NMR spectra were measured on a JEOL ECA 500 spectrometer at 298 K with 64 scans and 16,384 points for a spectral width of 15,024.04 Hz.

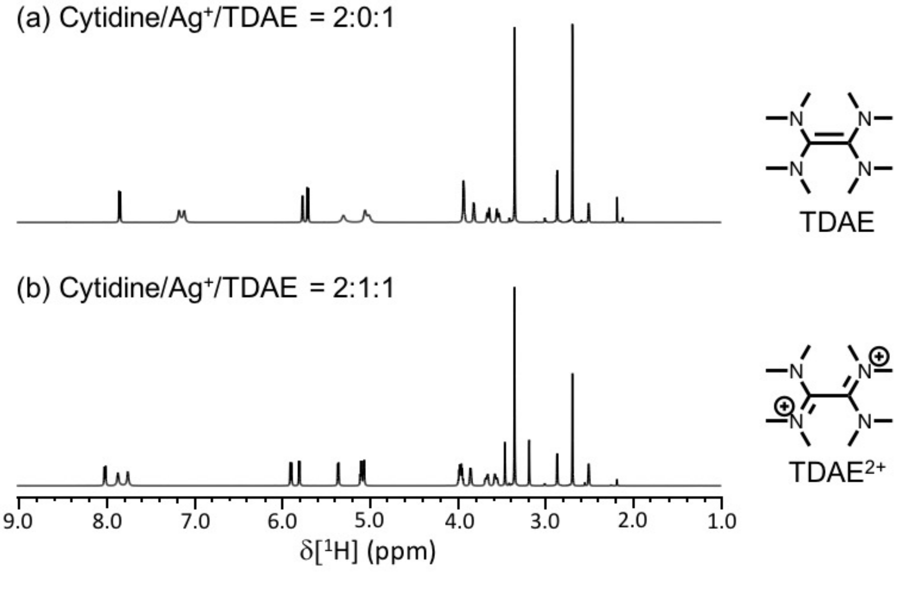

Fig. S7 1D ^{1}H NMR spectra (500 MHz) of (a) 60 mM cytidine/30 mM TDAE and (b) the supernatant fluid that was obtained from centrifuging the 60 mM cytidine/30 mM $AgNO_3$/30 mM TDAE in DMSO-d_6. In the presence of Ag^+, two new methyl proton signals appeared at 3.18 and 3.45 ppm. The 1D ^{1}H NMR spectra were measured by on a JEOL ECA 500 spectrometer at 298 K with 64 scans and 16,384 points for a spectral width of 15,024.04 Hz.

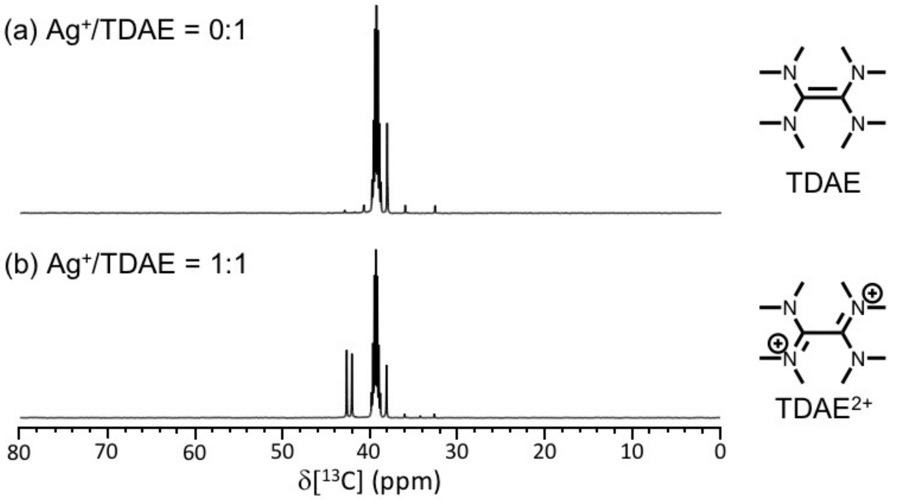

Fig. S8 ^{13}C NMR signals of the –N(Me)$_2$ carbons that were observed in the 1D ^{13}C NMR spectra (126 MHz) of (a) 240 mM TDAE and (b) the supernatant fluid that was obtained from centrifuging the 240 mM AgNO$_3$/240 mM TDAE solution in DMSO-*d*$_6$. In the presence of Ag$^+$, two new methyl carbon signals appeared at 42.1 and 42.7 ppm. The 1D ^{13}C NMR spectra were measured on a JEOL ECA 500 spectrometer at 298 K with 2,048 scans and 32,768 points for a spectral width of 47,348.48 Hz.

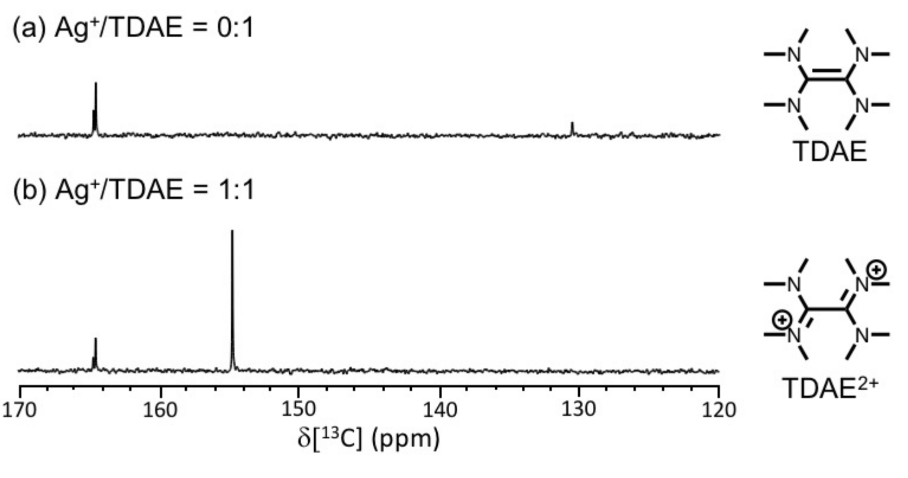

Fig. S9 ^{13}C NMR signals that were observed in the 1D ^{13}C NMR spectra (126 MHz) of (a) 240 mM TDAE and (b) the supernatant fluid that was obtained from centrifuging the 240 mM AgNO$_3$/240 mM TDAE solution in DMSO-*d*$_6$. In the presence of Ag$^+$, a new carbon signal appeared at 154.7 ppm. The 1D ^{13}C NMR spectra were measured on a JEOL ECA 500 spectrometer at 298 K with 2,048 scans and 32,768 points for a spectral width of 47,348.48 Hz.

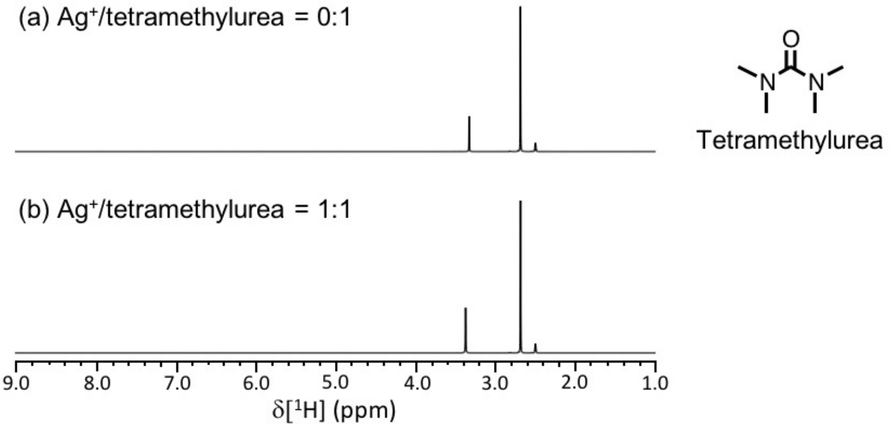

Fig. S10 1D ^{1}H NMR spectra (500 MHz) of (a) 30 mM tetramethylurea and (b) 30 mM $AgNO_3$/30 mM tetramethylurea in DMSO-d_6. The methyl proton signals of tetramethylurea were observed at 2.69 ppm. The 1D ^{1}H NMR spectra were measured on a JEOL ECZ 500 spectrometer at 298 K with 64 scans and 16,384 points for a spectral width of 15,024.04 Hz.

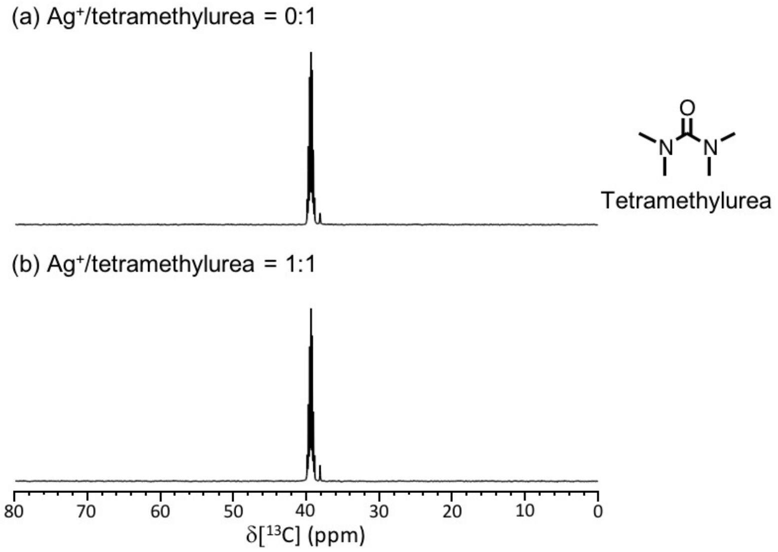

Fig. S11 ^{13}C NMR signals of the –N(Me)$_2$ carbons that were observed in the 1D ^{13}C NMR spectra (126 MHz) of (a) 30 mM tetramethylurea and (b) 30 mM $AgNO_3$/30 mM tetramethylurea in DMSO-d_6. The methyl carbon signal of tetramethylurea was observed at 38.1 ppm. The 1D ^{13}C NMR spectra were measured on a JEOL ECA 500 spectrometer at 298 K with 512 scans and 16,384 points for a spectral width of 41,118.42 Hz.

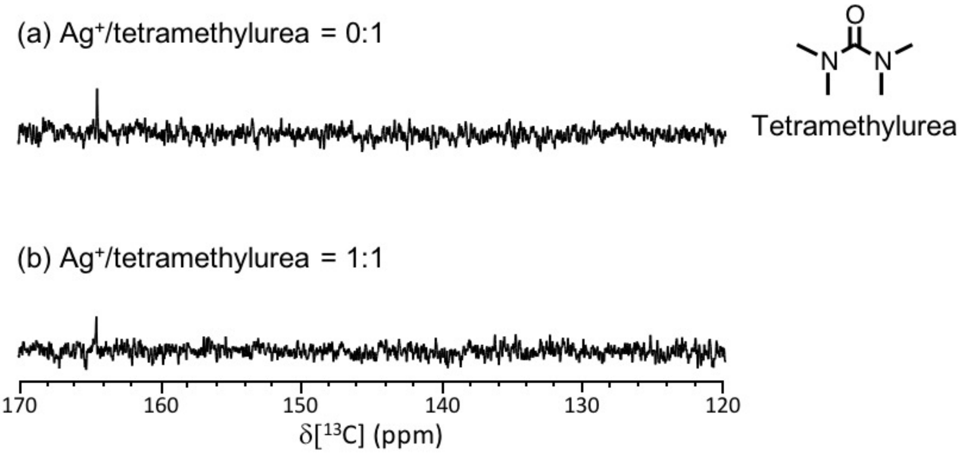

Fig. S12 ^{13}C NMR signals of the C=O carbon, as observed in the 1D ^{13}C NMR spectra (126 MHz) of (a) 30 mM tetramethylurea and (b) 30 mM $AgNO_3$/30 mM tetramethylurea in DMSO-d_6. The C=O carbon signal of tetramethylurea was observed at 164.5 ppm. The 1D ^{13}C NMR spectra were measured on a JEOL ECA 500 spectrometer at 298 K employing 512 scans and 16,384 points for a spectral width of 41,118.42 Hz.

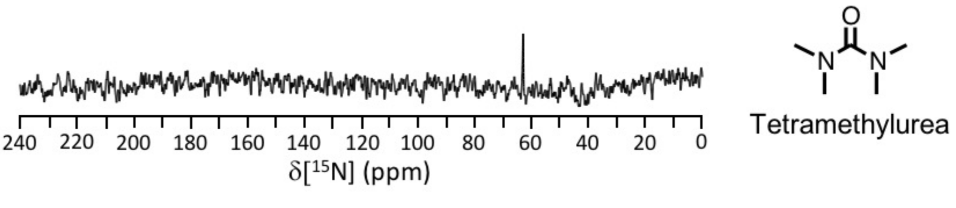

Fig. S13 1D ^{15}N NMR spectrum (51 MHz) of 1 M tetramethylurea in DMSO-d_6. The –$N(Me)_2$ nitrogen signal of tetramethylurea was observed at 63.1 ppm. The measurements were performed at 298 K utilising 28,902 scans and 32,768 points for a spectral width of 25,406.5 Hz.

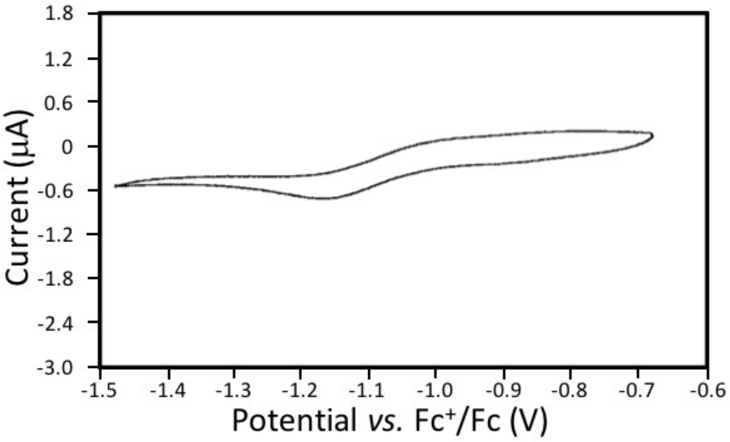

Fig. S14 Cyclic voltammogram of 30 mM tetramethylurea in DMSO containing 100 mM $NaNO_3$ as the supporting electrolyte. The scan rate was 0.01 V s^{-1}.